FEATURES OF NEUTRON IRRADIATION EFFECT ON DYNAMIC ACOUSTO-DEFECT INTERACTION IN SILICON SOLAR CELLS

O.YA. OLIKH

Taras Shevchenko National University of Kyiv, Faculty of Physics
(64, Volodymyrska Str., Kyiv 01601, Ukraine)

PACS 43.35.Ty
©2010

The effect of ultrasound on the electron diffusion length and the short-circuit current in silicon solar cells operating in the dynamic mode has been studied experimentally. The variations of features of this effect after a modification of semiconductor structures by the neutron irradiation are analyzed. It is shown that a reversible reconstruction of defect complexes in the ultrasound field can be responsible for the effects observed.

1. Introduction

Ultrasound is known to interact actively with defects in a crystal lattice owing to the elastic and electric fields associated with them [1–6]. As a consequence, the ultrasound wave action may give rise to the appearance of new properties or a substantial modification of existing ones in semiconductor crystals, structures, or devices. In other words, ultrasound can be used as an active tool of the so-called defect engineering, a physico-technological trend that has been actively developed recently [7]. In particular, rather promising is the creation of the element base for new-generation electronics, which is based on the controllable dynamic formation of active centers and nanoclusters.

At the same time, the issue of acousto-defect interactions in semiconductors belonging to the silicon and germanium types has not been studied enough. Not only does a complete theory of this phenomenon not exist, but there is also the lack of experimental data which would allow one to predict the precise character of acoustically induced variations in substance properties. On the other hand, it is clear that the properties of the defect subsystem of a crystal, together with the parameters of ultrasound waves, are crucial for such phenomena. The material irradiation is one of the well-studied tools for affecting this subsystem. Therefore, in order to obtain new information that would allow us to improve our understanding of the processes occurring in semiconductor crystals at ultrasound propagation, it seems reasonable to compare the features of acoustically induced phenomena in structures, the defect compositions of which differ because of the irradiation influence, in particular, due to the irradiation by neutrons.

This work presents the results of experimental studies of the effect of ultrasound on the parameters of silicon solar cells (the short circuit current and the electron diffusion length) before and after their modification by neutron irradiation. In contrast to the overwhelming majority of papers which were devoted to acoustically induced phenomena in semiconductors and to the irreversible (static) changes of properties of crystals or structures due to the ultrasound treatment, we aimed at researching the dynamic (reversible) effects which arose only during a ultrasound loading (UL) and disappeared after its termination. Actually, an opportunity to make a dynamic acoustic control over a photo-electric converter was examined. Probable mechanisms of acoustically induced phenomena in non-irradiated and neutron-irradiated structures have also been analyzed.

2. Experimental Specimens and Technique

2.1. Specimens

Solar cells (SCs) were fabricated on the basis of Cz p-Si substrates of the thickness $d_{\mathrm{p}} = 300$ μm doped with boron to the concentration $p = 1.25 \times 10^{15}$ cm^{-3}. A conductive layer of the thickness $d_n \approx 0.5$ μm and with

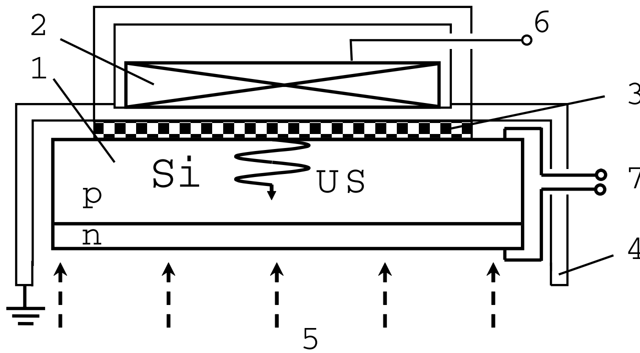

Fig. 1. The scheme of experimental chamber: (*1*) solar cell, (*2*) piezoelectric converter, (*3*) dielectric layer, (*4*) screen, (*5*) monochromatic light, (*6*) contact for supplying high-frequency voltage for ultrasound excitation, (*7*) contacts for CVC measurements

the electron-type conductivity ($n \approx 10^{19}$ cm^{-3}) was created on the substrate surface by implanting phosphorus ions. Aluminum contacts were deposited on the SC surfaces: a continuous one on the p-region and a contact grid on the n-region. The specimen surface area S was approximately equal to 1 cm^2.

Some structures were irradiated with reactor neutrons characterized by a wide energy spectrum (Institute for Nuclear Research of the NASU, Kyiv). The total neutron fluence was 4×10^{11} cm^{-2}. Below, the notations SCO and SCN will be used for irradiated and non-irradiated solar cells, respectively.

2.2. Measurement technique

The structures to study were arranged in a chamber (Fig. 1), and their current-voltage characteristics (CVCs) were measured. For this purpose, we used a special computer-assisted installation on the basis of an ADA-1282 analog-to-digital converter which allowed direct and reverse CVC branches to be measured in the dc range from 3×10^{-10} to 10^{-2} A with a bias voltage increment of 0.01 V. Measurements were carried out under the following conditions:

(i) Under the monochromatic illumination of specimens from the n-layer side. For this purpose, we used light with a wavelength of 900 or 950 nm, obtained with the use of an UM-2 monochromator. Depending on experimental conditions, the illumination intensity for a specimen $W_{\rm ph}$ was changed by a factor of 20. A preliminary calibration $W_{\rm ph}$ was carried out with the help of a 9E111A germanium photodiode.

(ii) When the specimens were acoustically loaded. For UL, we used $\rm LiNbO_3$ piezoelectric transducers which allowed us to excite longitudinal waves with the frequency $f_{\rm US} = 8.0$ or 26.1 MHz. The intensity of acoustic waves in the specimen, $W_{\rm US}$, depended on the amplitude $U_{\rm RF}$ of the high-frequency voltage supplied to a piezoelectric transducer. Its value was estimated with the help of the relation [8] $W_{\rm US} = 4k^2 C_{\rm p} f_{\rm US} Z_{\rm p} U_{\rm RF}^2/(Z_{\rm Si} S_{\rm p} M_0)$, where k is the coefficient of electromechanical coupling; $C_{\rm p}$ and $S_{\rm p}$ are the capacitance and the area of a piezoelectric transducer, respectively; $Z_{\rm p}$ and $Z_{\rm Si}$ are the acoustic impedances of lithium niobate and silicon, respectively; and M is a coefficient which is determined by the transducer resonance and antiresonance frequencies. When estimating the intensity, the circumstance that the thicknesses of the screening and dielectric layers were much less than the quarter wavelength was taken into account. In this work, we applied acoustic waves with $W_{\rm US}$ up to 0.8 W/cm^2, which corresponds to the mechanical stress $\sigma_{\rm US} = \sqrt{2W_{\rm US}\rho_{\rm Si} v_{\rm US}} = 5.4 \times 10^5$ N/m^2, where $\rho_{\rm Si}$ is the silicon density, and $v_{\rm US}$ the sound speed in silicon. As is seen from Fig. 1, the chamber design provided the piezoelectric transducer screening, which ensured the electric independence between measurements of CVC and the ultrasound excitation.

In the course of experiments, the specimen temperature was monitored using a copper–constantan thermocouple. The specimens were heated up both during UL and with the help of special resistive heaters which are not shown in Fig. 1. In the latter case, the specimen temperature was changed in the range from 290 to 330 K.

2.3. Parameter determination procedure

The measured CVCs were used to determine the short circuit current (SCC) $I_{\rm SC}$ and the electron diffusion length in the p-region L_n for SCO and SCN under UL, as well as without sound. The SCC was determined following a standard routine by the intersection of the CVC plot and the axis of currents. Concerning L_n, we used the following procedure.

When a solar cell is illuminated by monochromatic light from the n-layer side, and light is mainly absorbed in the diode base depth (in the p-region), the value of SCC is described by the expression [9]

$$I_{\rm SC} = \frac{W_{\rm ph}(1-R)\,q\beta S\lambda}{hc}\frac{\alpha L_n}{1+\alpha L_n}\,, \qquad (1)$$

where R is the reflection coefficient for the specimen surface, q the elementary charge, β the coefficient of quantum yield, h Planck's constant, c the light speed in vacuum, and α the coefficient of light absorption. Therefore, $I_{\rm SC}$ depends linearly on the number of photons

$N_{\rm ph} = W_{\rm ph}\lambda/hc$ falling on the surface per time unit. We have

$$I_{\rm SC} = KN_{\rm ph}\,, \tag{2}$$

where $K = \frac{(1-R)\,q\beta S\alpha L_n}{1+\alpha L_n}$ is the proportionality factor. Knowing the coefficients K_1 and K_2 for two close wavelengths λ_1 and λ_2, respectively, one can determine L_n:

$$L_n = \frac{(K_1\alpha_2)/(K_2\alpha_1) - 1}{\alpha_2(1 - K_1/K_2)}\,, \tag{3}$$

where α_1 and α_2 are the absorption coefficients for light with wavelengths λ_1 and λ_2, respectively. When deriving expression (3), the quantities R and β were considered identical for both wavelengths.

For Si at $T = 300$ K, $\alpha_1 \approx 3.06 \times 10^2$ cm^{-1} for light with $\lambda_1 = 900$ nm, and $\alpha_2 \approx 1.57 \times 10^2$ cm^{-1} for light with $\lambda_2 = 950$ nm [10]. The data of the cited work concern intrinsic silicon. However, taking into account the fact that interband transitions take place at such photon energies, whereas the doping level is insufficient for the semiconductor to be degenerate, it seems reasonable to apply those values in our case as well. Hence, for both wavelengths, the effective absorption depth is much larger than d_n and the $p{-}n$-transition width d_{pn}; the latter is about 0.9 μm for structures under consideration. In addition, the experimentally measured dependences $I_{\rm SC} = f(N_{\rm ph})$ are really linear (see Fig. 2). Therefore, the use of formula (1) is completely justified in our case. For the given spectral range, the reflection coefficient depends rather weakly on the wavelength [10, 11], and $\beta = 1$ [12]. All this gives grounds for a practical application of formula (3). Therefore, the diffusion length was determined in this work on the basis of experimentally measured dependences $I_{\rm SC} = f(N_{\rm ph})$ for illumination wavelengths of 900 and 950 nm.

The intrinsic absorption coefficient is known to depend on the temperature at indirect transitions. Its temperature dependence can be described by the expression [13]

$$\alpha \sim \sum_{\substack{i=1,2\\ j=1,2}} C_i A_j \left(\frac{(hc/\lambda - E_{gj}(T) + E_{p\,i})^2}{\exp(E_{p\,i}/kT) - 1} + \frac{(hc/\lambda - E_{gj}(T) - E_{p\,i})^2}{1 - \exp(-E_{p\,i}/kT)} \right), \tag{4}$$

where $E_{p1} = 1.827 \times 10^{-2}$ eV and $E_{p2} = 5.773 \times 10^{-2}$ eV are the Debye frequencies of transverse optical and acoustic phonons, respectively; $C_1 = 5.5$, $C_2 = 4.0$, $A_1 = 3.231 \times 10^2$ cm^{-1}eV^{-2}, and $A_2 = 7.237 \times 10^3$ cm^{-1}eV^{-2} are constants. The temperature dependences $E_{g1}(T)$ and $E_{g2}(T)$ are described by the expression

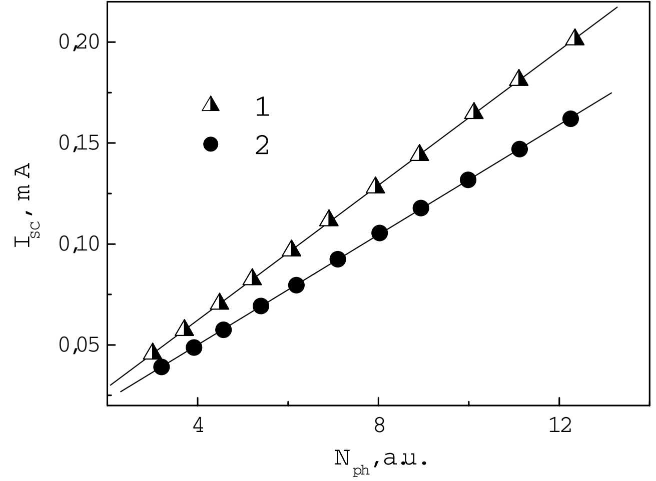

Fig. 2. Dependences of short circuit current for SCO on the number of photons falling on unit surface per unit time: points correspond to experimental data for $\lambda = 900$ (*1*) and 950 nm (*2*); lines show their linear approximation. $T = 290$ K

$$E_{gj}(T) = E_{gj}(0) - \frac{\gamma\,T^2}{T + \beta} \tag{5}$$

where $E_{g1}(0) = 1.1557$ eV, $E_{g2}(0) = 2.5$ eV, $\beta = 1108$ K, and $\gamma = 7.021 \times 10^{-4}$ eV/K^2 [13]. The calculations according to expression (4) showed that the parameter α_1 has to change from 2.99×10^2 to 3.32×10^2 cm^{-1}, and the parameter α_2 from 1.54×10^2 to 1.71×10^2 cm^{-1} in the temperature interval from 290 to 340 K.

3. Experimental Results

Our researches showed that the soundless heating of SCs, both irradiated and non-irradiated, is accompanied by an insignificant growth of $I_{\rm SC}$. This dependence is linear in the examined temperature interval,

$$I_{\rm SC}(T) = I_{\rm SC,\,0}[1 + \eta\,(T - T_0)]\,, \tag{6}$$

where $I_{\rm SC,0}$ is the SCC at the temperature $T_0 = 290$ K, and η is the temperature coefficient. For SCO, $I_{\rm SC,0} = 0.16$ mA and $\eta = 5.3 \times 10^{-3}$ K^{-1}; for SCN, $I_{\rm SC,0} = 0.17$ mA and $\eta = 4.5 \times 10^{-3}$ K^{-1}. Note that, in general, the SCC value decreased after irradiation. Therefore, to increase the relative accuracy of its determination at SCN studies, illumination approximately twice as

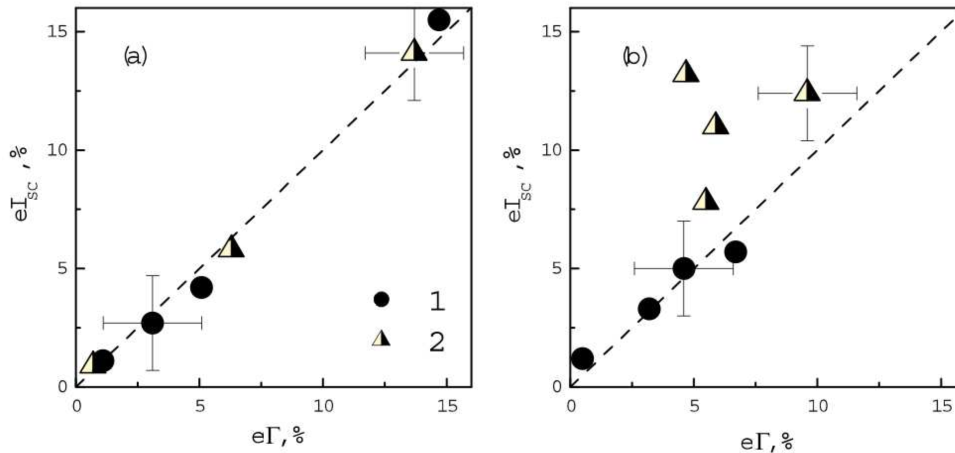

Fig. 3. The relative variation of short circuit current versus the variation of minority charge carrier diffusion length at soundless heating (*a*) and under UL conditions (*b*) in non-irradiated (*1*) and irradiated (*2*) structures. $I_{\rm SC}$ was determined for illumination with $\lambda = 900$ nm

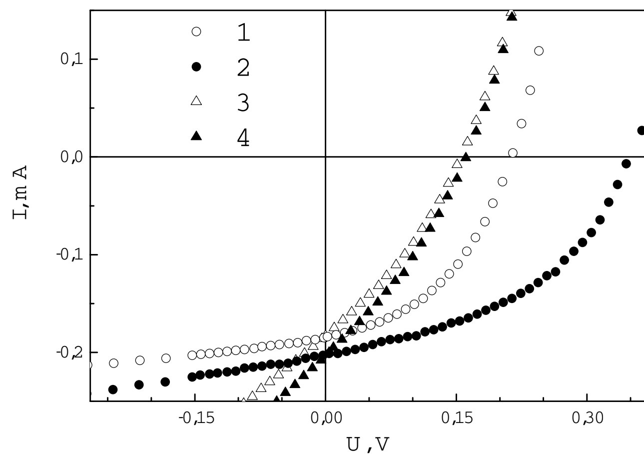

Fig. 4. CVCs of non-irradiated (*1*, *2*) and irradiated (*3*, *4*) SCs under (*2*, *4*) and not under (*1*, *3*) UL conditions: $T = 319$ (*1*, *2*) and 305 K (*3*, *4*); $f_{\rm US} = 8$ (*2*) and 26 MHz (*4*); $\sigma_{\rm US} = 5.4 \times 10^5$ (*2*) and 1.7×10^5 N/m^{-2} (*4*); $\lambda = 900$ nm . $W_{\rm ph}$ is different for SCN and SCO

intense as that used for SCO studies was used, provided that all other conditions were identical.

Such an SCC increment is associated [9] with an increase of L_n at the temperature growth. To verify this hypothesis, we determined the diffusion length in the whole temperature interval under investigation. It turned out that the temperature growth is really accompanied by an increase of L_n, and the increment of $I_{\rm SC}$ can be explained almost completely by this process. In Fig. 3,*a*, a diagram is presented, where the SCC changes at different temperatures are reckoned along the vertical axis, and the variations of the coefficient $\Gamma = \alpha L_n/(1 + \alpha L_n)$ along the horizontal one. The latter values were calculated, by using L_n-values determined for the temperatures, at which $I_{\rm SC}$ was measured, and by taking the temperature dependence of the absorption coefficient (4) into account. The figure demonstrates relative variations of $I_{\rm SC}$ and Γ with respect to their values at T_0. According to expression (1), if R and β depend weakly on the temperature, it is the coefficient Γ that governs the SCC variation. Really, the $I_{\rm SC}$- and Γ-variations are almost identical for irradiated and non-irradiated structures (points in Fig. 3,*a* are located very close to the diagonal).

Before proceeding to the consideration of the ultrasound influence on the quantities concerned, we would like to emphasize that all detected acoustically induced (AI) variations of parameters were reversible; i.e. after the UL had been stopped, the SC parameters became restored to their initial values within the interval of about 10 min. We did not manage to study transient processes in detail, because the CVC measurement time was comparable with the relaxation one.

Under UL, both SCO and SCN specimens changed their CVCs (see Fig. 4). In particular, the SCC grows under UL (see Fig. 5). Since UL gives rise to a certain heating of specimens and the $I_{\rm SC}$-magnitude depends on the temperature, we used the relative variation of SCC $\varepsilon I_{\rm SC} = (I_{\rm SC}^{\rm US} - I_{\rm SC}^{T})/I_{\rm SC}^{T}$ as a criterion of the AI influence. Here, $I_{\rm SC}^{\rm US}$ is the SCC value measured in the course of the acoustic loading of the structure approximately in 40 min after its start in the stationary temperature mode, and

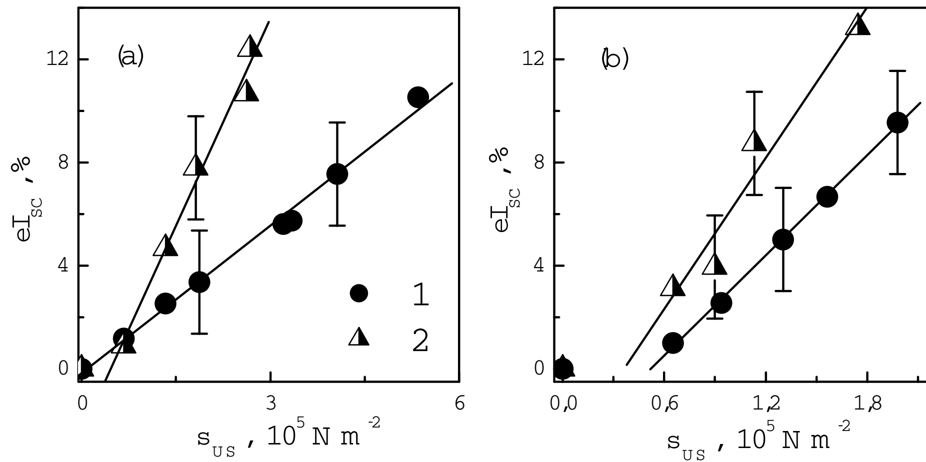

Fig. 5. Dependences of acoustically induced SCC changes on the strain in the ultrasonic wave in non-irradiated (*1*) and irradiated (*2*) structures: $f_{\rm US} = 8$ (*a*) and 26 MHz (*b*); $I_{\rm SC}$ was determined for illumination with $\lambda = 900$ nm

$I^T_{\rm SC}$ is the SCC value in the absence of ultrasound in the SC, provided that the SC temperature is equal to that during UL. On the basis of reported results, the following features of the acoustic influence on SCC can be marked: 1) the quantity $\varepsilon I_{\rm SC}$ grows almost linearly with $\sigma_{\rm US}$; 2) ultrasound with higher frequencies changes the SCC more efficiently; 3) the AI effect is more pronounced in irradiated specimens.

Among probable reasons for an AI increase of SCC, there is the growth of L_n in the acoustic field. For checking this assumption, we carried out measurements of the diffusion length under UL conditions. It turned out that, really, the magnitude of L_n is larger at the acoustic wave propagation than in the absence of UL at the same temperature. The AI growth of the diffusion length is about 100 μm by an order of magnitude for the largest $\sigma_{\rm US}$ that were used, and it was observed for both SCO and SCN specimens. By the way, the effects of an AI dynamic increase of L_n in *p*-Si were observed earlier as well [14].

Our estimations testify that the SCC growth in non-irradiated specimens can be almost completely connected with the AI influence on the diffusion length (see Fig. 3,*b*). The mechanism of this phenomenon can be as follows. It is known that the impurity complex $\rm B_SO_{2\it i}$ is one of the main recombination centers that govern the diffusion length of minority charge carriers in Cz Si:B which is the material the SC substrate is made of [15, 16]. A charge-dependent configuration bistability is characteristic of this defect: it can be located in either the configuration $\rm B_SO^{\it sq}_{2\it i}$ which is more probable for the singly charged positive state or in the configuration $\rm B_SO^{\it st}_{2\it i}$ which is more probable for the neutral state of the complex. In work [4], it was demonstrated that 1) just $\rm B_SO_{2\it i}$ complexes are present in the structures that are similar by composition to those used in this work; 2) point defects change their recombination activity under UL conditions, in particular, the possibility of the AI reconstruction of $\rm B_SO^{\it sq}_{2\it i}$ center has been considered. In our opinion, in the case concerned, just this reconstruction, $\rm B_SO^{\it sq}_{2\it i} \longrightarrow B_SO^{\it st}_{2\it i}$, of some complexes takes place during UL, which stimulates, afterwards, their transition into the neutral state. As a result, the recombination activity of $\rm B_SO_{2\it i}$ decreases, and L_n and $I_{\rm SC}$ grow. As is seen from the given dependences (Fig. 5), the efficiency of such a reconstruction depends linearly on the mechanical stress in the ultrasound wave. An enhancement of the efficiency of AI changes with increase in the ultrasound frequency, which is observed in experiments, can be connected with the approach of $f_{\rm US}$ to the characteristic frequencies of impurity complex vibrations, i.e. with the known resonance character of acousto-defect interactions [5]. A certain argument that it is the reconstruction of defects that induces the AI changes shown in Fig. 5 is a rather slow, during ten minutes, restoration of parameters to their initial values after UL stops.

At the same time, our researches showed that, for neutron-irradiated specimens, the SCC change under UL conditions is larger than the variations of the coefficient Γ connected with the AI growth of L_n (Fig. 3,*b*). This fact testifies to the existence of additional mechanisms of ultrasound influence on SCC in such specimens. As is seen from expression (1), a reduction of the reflection

coefficient for the specimen surface can be one of the origins.

Work [6] reported on the results which evidence a reduction of R in the spectral range used in our experiments after the ultrasound treatment of silicon. However, we have to notice that this effect has a residual character, and the authors of work [6] associated it with a reduction of the doping impurity concentration in the near-surface layer of the semiconductor owing to the AI diffusion into the crystal depth. In our experiments, we used acoustic waves with a considerably lower power than that in work [6]: 0.8 and 5 W/cm^2, respectively. Therefore, the AI diffusion of phosphorus did not occur, and SCC in SCO specimens grew only as a result of a change of the carrier diffusion length owing to the AI reconstruction of B_SO_{2i}.

The defect composition of the near-surface layer is known (see, e.g., work [17]) to substantially affect the processes of light reflection. In our opinion, the defects formed as a result of the neutron irradiation (first of all, vacancies and vacancy-containing complexes) are acoustically active, i.e. they can change their state at the interaction with elastic vibrations. In particular, it was shown in work [1] that a dynamic modification of a vacancy–oxygen complex takes place in Cz-Si in the ultrasound field. It is a similar AI reconstruction or a change of the level population in complexes during UL that gives rise to a reduction of the reflection coefficient and the appearance of an additional mechanism for the SCC growth. By the way, such processes – namely, the reduction of R down to 8% owing to a change of the level population in the course of acoustic loadings – were observed earlier in epitaxial GaAs films [18]. A certain texturing of the surface of neutron-irradiated structures under UL conditions can be another reason for the reduction of R.

Therefore, the neutron irradiation can induce a spatial rearrangement of the region with the effective acousto-defect interaction, so that these processes start to effectively run in the near-surface layer of a semiconductor as well.

4. Conclusions

The experimental research of the ultrasound influence in the dynamic regime on the short circuit current and the diffusion length of minority charge carriers in non-irradiated and neutron-irradiated silicon solar cells has been carried out. The acoustically induced reversible growth of those parameters has been revealed. The characteristic features of their dependences on the ultrasound frequency and the mechanical stress in an acoustic wave have been studied.

It has been demonstrated that the prevailing mechanism of SCC growth in non-irradiated structures is an increase of the charge carrier diffusion length, which can take place, in its turn, owing to the reconstruction of impurity complexes B_SO_{2i}. In the neutron-irradiated structures, an additional mechanism of acoustically induced influence on SCC can appear. It can be associated with a reduction of the light reflection coefficient at the cell surface, e.g., owing to the modification of vacancy complexes.

The author is grateful to Prof. A.V. Sachenko for useful discussions and remarks.

1. Ya.M. Olikh, N.D. Timochko, and A.P. Dolgolenko, Pis'ma Zh. Tekh. Fiz. **32**, 67 (2006).

2. A. Romanyuk, V. Spassov, and V. Melnik, J. Appl. Phys. **99**, 034314 (2006).

3. A. Davletova and S.Zh. Karazhanov, J. Phys. D **41**, 165107 (2008).

4. O.Ya. Olikh, Fiz. Tekh. Poluprovodn. **43**, 774 (2009).

5. Ya.M. Olikh and Yu.N. Shavlyuk, Fiz. Tverd. Tela **38**, 3365 (1996).

6. B.N. Zaveryukhin, N.N. Zaveryukhina, and O.M. Tursunkulov, Pis'ma Zh. Tekh. Fiz. **28**, 1 (2002).

7. L.S. Smirnov, Fiz. Tekh. Poluprovodn. **35**, 1029 (2001).

8. D. Royer and E. Dieulesaint, *Elastic Waves in Solids: Applications to Signal Processing* (Springer, New York, 1999).

9. A.L. Fahrenbruch and R.H. Bube, *Fundamentals of Solar Cells: Photovoltaic Solar Energy Conversion* (Academic Press, New York, 1983).

10. M.A. Green and M. Keevers, Prog. Photovolt. **3**, 189 (1995).

11. H.R. Philipp and E.A. Taft, Phys. Rev. **120**, 37 (1960).

12. V.I. Gaman, Physics of Semiconductor Devices (Tomsk Univ., Tomsk, 1989) (in Russian).

13. *Practical Handbook of Photovoltaics. Fundamentals and Applications*, edited by T.Markvart and L.Castaner (Elsevier, Amsterdam, 2003).

14. O.Ya. Olikh, Fiz. Tverd. Tela **44**, 1198 (2002).

15. J. Schmidt, K. Bothe, D. Macdonald, J. Adey, R. Jones, and D.W. Palmer, J. Mater. Res. **21**, 5 (2006).

16. J. Adey, R. Jones, D.W. Palmer, P.R. Briddon, and S. Oberg, Phys. Rev. Lett. **93**, 055504 (2004).

17. V.A. Kizel, *Light Reflection* (Nauka, Moscow, 1973) (in Russian).

18. O.O. Korotchenkov and O.M. Antonov, Ukr. Fiz. Zh. **39**, 667 (1994).

Received 22.04.10.
Translated from Ukrainian by O.I. Voitenko

ОСОБЛИВОСТІ ВПЛИВУ НЕЙТРОННОГО ОПРОМІНЕННЯ НА ДИНАМІЧНУ АКУСТО-ДЕФЕКТНУ ВЗАЄМОДІЮ У КРЕМНІЄВИХ СОНЯЧНИХ ЕЛЕМЕНТАХ

О.Я. Оліх

Р е з ю м е

У роботі експериментально досліджено вплив ультразвуку на довжину дифузії електронів та струм короткого замикання кремнієвих сонячних елементів у динамічному режимі. Проаналізовано зміни особливостей акустоіндукованого впливу після модифікації напівпровідникових структур шляхом нейтронного опромінення. Показано, що причинами ефектів, які спостерігаються, може бути оборотна перебудова дефектних комплексів в ультразвуковому полі.